Reports

Mineralogic Evidence for an Impact Event at the Cretaceous-Tertiary Boundary

Abstract. *A thin claystone layer found in nonmarine rocks at the palynological Cretaceous-Tertiary boundary in eastern Montana contains an anomalously high value of iridium. The nonclay fraction is mostly quartz with minor feldspar, and some of these grains display planar features. These planar features are related to specific crystallographic directions in the quartz lattice. The shocked quartz grains also exhibit asterism and have lowered refractive indices. All these mineralogical features are characteristic of shock metamorphism and are compelling evidence that the shocked grains are the product of a high velocity impact between a large extraterrestrial body and the earth. The shocked minerals represent silicic target material injected into the stratosphere by the impact of the projectile.*

Ever since Alvarez *et al.* (*1*) reported finding an anomalously high amount of iridium in a marine clay layer at the Cretaceous-Tertiary (K-T) boundary at Gubbio, Italy, a worldwide search for similar anomalies at this boundary has proceeded apace. At a recent conference on large-body impacts, Alvarez *et al.* (*2*) listed 32 sites that exhibited anomalies in seven countries and two ocean basins. All but two of these anomalies were discovered in marine rocks; the two nonmarine sites were found in continental deposits of the Raton Basin in New Mexico (*3*). The location of iridium anomalies at the K-T boundary in rocks representative of continental environments was crucial to the extraterrestrial impact theory, because now these anomalies cannot be attributed to a peculiarity of oceanic processes (*4*).

Most of the studies on the K-T boundary sections have been directed at elucidating the amounts and ratios of the platinum group metals and other trace elements. In 1980, two of us decided that the best evidence of an extraterrestrial impact would lie in the mineralogy of the boundary clay layer, much as the proof of the volcanic origin of tonsteins (widespread layers of altered volcanic ash in coal beds) had been decided by mineralogical analyses (*5*). In 1982, an unusual thin claystone layer at the base of the lowest lignite in the Tullock Member of the Fort Union Formation (Paleocene) near Brownie Butte in Garfield County, east-central Montana, was discovered (*6*). This claystone (1 to 1.5 cm thick) contains iridium at 1.00 parts per billion (ppb), a value some 200 times greater than local background values (*7*).

The claystone layer is located exactly at the K-T palynological boundary. Palynomorphic analyses (*8*) of the 5-cm thick lignite immediately overlying the claystone layer revealed a good Paleocene assemblage, including: *Ulmipollenites, Kurtzipites, Pandaniidites, Alnipollenites*, and *Ovoidites*. A sample of carbonaceous shale taken immediately below the claystone layer contained an excellent late Cretaceous palynomorphic assemblage, including: *Pandaniidites, Alnipollenites, Proteaccidites, Kurtzipites, Wodehouseia spinata, Aquilapollenites* (several species, many specimens), *Ulmipollenites, Cranwellia, Liliacidites*, and *Balmeisporites*. In the lignite above the claystone layer, a palynomorph count yielded 48 percent angiosperm pollen, 52 percent fern spores. A similar count in the carbonaceous shale immediately below the claystone layer revealed 83 percent angiosperm pollen, 17 percent fern spores. Thus, the disappearance of the Cretaceous marker pollens *Proteacidites* and *Aquilapollenites* and the abrupt increase in the fern to angiosperm ratio across the claystone layer places the latter exactly on the K-T boundary, and is comparable to palynomorph changes reported at this boundary in the Raton Basin (*3*).

The claystone layer itself is hard, pink when moist, and extremely fine grained, with a blocky to conchoidal fracture. It becomes plastic when pulverized and added to water. The claystone is remarkably clean, with only occasional organic fragments and some tiny, tan, subspherical bodies scattered through it. In the scanning electron microscope, fracture surfaces of this claystone reveal an unusual texture of microspheroidal particles 0.3 to 1 μm in diameter composed of kaolinite. In contrast, thin, altered tuffs (tonsteins) in lignite or coal throughout the Rocky Mountain region of the western United States are nonplastic, are much coarser grained with a rougher fracture, and have a microtexture consisting of platelets or vermicules of well crystallized kaolinite.

Bulk analysis of the Brownie Butte claystone sample by x-ray diffraction results in a pattern of peaks representing equal parts of poorly crystallized kaolinite and smectite plus some minor quartz. Results of more detailed clay mineralogical studies on this sample have been presented (*9*).

The clay mineral fraction was removed by washing with water after dispersal with a peptizing agent and ultrasonic treatment. Some aggregate grains of clay minerals that were the same size as the quartz grains (75 to 100 μm) remained after this treatment, so they were removed by treating the sample with hydrofluoric acid (HF) until the clay grains were dissolved (about 6 minutes). The nonclay mineral fraction amounted to about 0.01 percent (by weight) of the total sample. Almost 90 percent of this residue was quartz, and another 2 percent was sanidine.

This HF treatment etched the quartz grain surfaces. When individual quartz grains from the residue were examined in a scanning electron microscope (SEM), prominent lamellar features (Fig. 1A) were revealed, occurring as multiple intersecting sets in about 25 percent of the grains. Unetched quartz grains from the Brownie Butte sample did not exhibit these features. Etched quartz grains from tonsteins of volcanic origin in the Brownie Butte area and from elsewhere in the western United States do not exhibit these features. When viewed under a polarizing microscope, these lamellar features in unetched grains from the boundary layer are seen to be planar, with the planes extending throughout the grain. Some material more soluble than the quartz (probably a glassy phase) was selectively removed by the acid, bringing the lamellae into prominence when viewed in the SEM. We later discovered that others had studied replicated surfaces of HF-etched, shocked quartz grains in a transmission electron microscope and observed similar planar lamellae (*10*).

These planar features are not unique to this K-T boundary claystone. Indeed, they appear to be directly analogous to shock metamorphic features in rocks associated with meteorite impact craters,

Table 1. Refractive indices of 15 quartz grains from Brownie Butte, Montana, showing planar features.

Number of grains	n_o*	n_e*	$(n_o + n_e)/2$
Ideal quartz	1.544	1.553	1.5485
2	1.542	1.551	1.5465
1	1.541	1.551	1.546
4	1.541	1.550	1.5455
2	1.541	1.549	1.545
3	1.540	1.549	1.5445
1	1.540	1.548	1.544
2	1.537	1.546	1.5415

*Values are ±0.001.

which have been variously described as diaplectic quartz (*11*), shocked quartz (*12*), quartz with deformation lamellae (*13*), and shock lamellae or planar elements (*14*). Some workers have categorized these features according to their appearance and relationship to quartz crystallography (*15*), but we will consider them all together under the term "planar features." The critical facts about these planar features are their well-documented association with known impact structures and their diagnostic value as indicators of shock metamorphism.

In order to prove that these planar features are due to shock metamorphism and not tectonically derived, we measured their orientation relative to the c-axis of quartz by the spindle stage technique. In tectonically derived lamellae (so-called Böhm lamellae), the normals or poles to the planes occur only at low angles to the c-axis of the quartz; most occur at about 12° (*15*). Shock-induced planar features, on the other hand, have been shown by numerous workers to occur at discrete angles to the quartz c-axis, conforming to specific (*hkil*) crystal faces or planes in the lattice. Our measurements of planar features in the unetched quartz grains from the boundary claystone show the same crystallographic orientations as those found in shocked quartz from meteorite impact craters, nuclear explosions, and laboratory explosive shock experiments (*15, 16*). The ω $\{10\bar{1}3\}$ and π $\{10\bar{1}2\}$ crystallographic orientations of these features were prominent in our grains (Fig. 1B), as has been observed by others for shocked materials (*17*).

Figure 2 is a histogram of our results. Some of our grains had as many as seven different sets of planar features, whereas tectonically deformed quartz rarely has more than one set per grain. Also, the planar features in our sample do not look like Böhm lamellae, in that they are nearly straight and planar. Furthermore, mean refractive indices $(n_o + n_e)/2$ measured on the same grains mounted for crystallographic planar determinations ranged between 1.5465 and 1.5415 (Table 1). Reduced refractive indices have been shown to be characteristic of shock-metamorphosed quartz (*15*).

Further evidence of the shock-metamorphic origin of the quartz in the boundary layer can be derived from x-ray diffraction analysis. A single-crystal quartz grain displaying several sets of planar features was mounted in a Debye-Scherrer 114.6-mm camera and exposed to CuKα radiation. Under these diffraction conditions, lattice strains caused by shock pressures will cause streaking, or "asterism," of the sharp diffraction spots normally obtained from an unstressed, single-crystal quartz grain (*18*). Our quartz grain showed very noticeable asterism in its pattern, confirming its exposure to high shock pressures. The amount of asterism was not quantified, but visually it appears to be similar to that developed in laboratory experiments at 90 kilobars (kb) or more (*18*).

Very faint lines for stishovite, a high-pressure polymorph of SiO_2, were noticed in the x-ray pattern of the grain examined for asterism. In order to confirm this, we mounted ten grains displaying multiple planar features in a 114.6-mm Gandolfi camera and obtained a pattern also displaying very faint lines for stishovite. Finally, several milligrams of clay-free sample were treated with HF for 24 hours to remove quartz. Again, very faint lines for stishovite were evident in the Gandolfi pattern of this residue. In none of these x-ray patterns, however, were any of the diagnostic lines for coesite, another high-pressure SiO_2 polymorph, recognized.

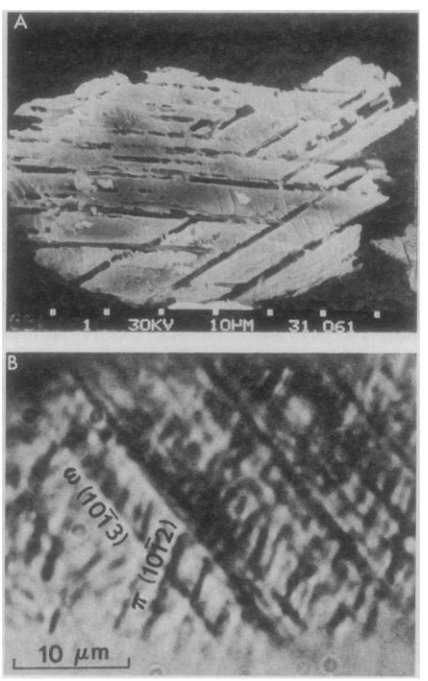

Fig. 1. Shock-metamorphosed quartz grains displaying planar features. (A) SEM micrograph of HF-etched grain, showing one minor and two major sets of planar features. Open planar features of the two major sets are believed to have been once filled with a glassy phase. Distance between tick marks equals 10 μm. (B) Photomicrograph of an unetched quartz grain in plane polarized light. Prominent intersecting planar features are indexed to the corresponding crystallographic planes in quartz.

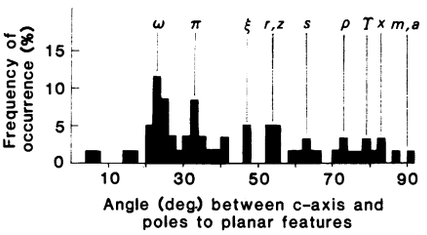

Fig. 2. Orientation with respect to the c-axis of the poles to 61 sets of planar features from 15 quartz grains, plotted at 2° intervals. Greek and Roman letters designate specific crystallographic planes in quartz.

In summary, all the evidence we have gathered on this claystone layer at Brownie Butte is consistent with its origin as fallout from the impact of a large, extraterrestrial body. The presence of quartz in this layer indicates the target material was at least partially silicic. We have had the claystone layer positioned exactly at the K-T boundary by palynology, and trace element analysis has shown that it contains an anomalous amount of iridium. More importantly, it contains shock-metamorphosed quartz with: (i) multiple sets of planar features indexing to specific crystallographic planes, (ii) reduced refractive indices, (iii) asterism, and (iv) traces of the high-pressure mineral stishovite. All of these latter features are characteristic of shocked quartz associated with known meteorite impact craters.

These same shock-metamorphic features should be sought at K-T boundary sites elsewhere. Their discovery at these other localities will constitute further proof that the boundary layer originated with a meteorite impact. Acceptance of this origin for the boundary layer will facilitate the evaluation of the influence of such an event on the contemporary flora and fauna and their numerous extinctions.

B. F. BOHOR
E. E. FOORD
P. J. MODRESKI
D. M. TRIPLEHORN
U.S. Geological Survey,
Box 25046,
Denver, Colorado 80225

References and Notes

1. L. W. Alvarez, W. Alvarez, F. Asaro, H. V. Michel, *Science* **208**, 1095 (1980).
2. W. Alvarez *et al.*, *Geol. Soc. Am. Spec. Pap. 190* (1982), pp. 305–315.
3. C. J. Orth *et al.*, *Science* **214**, 1341 (1981).
4. M. R. Rampino [*Geol. Soc. Am. Spec. Pap. 190* (1982), pp. 423–433] makes a case for concentration of iridium in marine clays at the K-T boundary by solution of pelagic limestones. This scenario cannot be applied to nonmarine boundary clays located in siliclastic rocks.
5. Altered volcanic tuffs in coal beds (tonsteins) have been extensively studied (by B.F.B. and D.M.T.) throughout the United States. Techniques for determining the original volcanic derivation of these claystones by whole sample analysis can be found in D. M. Triplehorn and B. F. Bohor [*U.S. Geol. Surv. Open-File Rept. 81-775* (1981)]; and B. F. Bohor and D. M. Triplehorn [*Guideb. Geol. Soc. Am. Annu. Coal Div. Field Trip* (1981), pp. 49–54].
6. The boundary claystone was found in the vicinity of a stratigraphic section near Brownie Butte described by R. H. Tschudy [*Geol. Soc. Am. Spec. Pap. 127* (1970), pp. 65–111].
7. Single-point instrumental neutron activation analysis of the claystone layer by C. J. Orth at Los Alamos Scientific Laboratories. Similar analyses by Orth of samples 30 cm above and below the boundary layer gave background values for iridium of 5.0 and 8.0 parts per trillion, respectively.
8. Palynologic analyses by R. H. Tschudy, U.S. Geological Survey, Denver, Colo.
9. B. F. Bohor, paper presented at the 20th Annual Meeting of the Clay Minerals Society, Buffalo, N.Y., October 1983.
10. C. B. Sclar, N. M. Short, G. G. Cocks, in *Shock Metamorphism of Natural Materials*, B. M. French and N. M. Short, Eds. (Mono Book, Baltimore, 1968), pp. 483–493.
11. W. v. Englehart and D. Stöffler, in *ibid.* pp. 159–168.
12. E. T. C. Chao, in *ibid.* pp. 135–158.
13. N. L. Carter, *Am. J. Sci.* **263**, 786 (1965).
14. D. Stöffler, *Fortschr. Mineral.* **49**, 50 (1972).
15. W. v. Englehart and W. Bertsch, *Contrib. Mineral. Petrol.* **20**, 203 (1969).
16. N. M. Short, in *Shock Metamorphism of Natural Materials*, B. M. French and N. M. Short, Eds. (Mono Book, Baltimore, 1968), pp. 185–210; F. Horz, in *ibid.* pp. 243–253.
17. T. E. Bunch, in *ibid.* pp. 413–432.
18. F. Dachille, P. Gigl, P. Y. Simons, in *ibid.* pp. 555–569; F. Horz and W. L. Quaide, *Lunar Planet. Sci. Inst. Contrib. 02* (1970).

19. We thank C. J. Orth and R. H. Tschudy for their analyses; E. Shoemaker, B. French, D. Stöffler, and A. Gratz for their helpful comments; and C. Sanderson for laboratory assistance.

24 January 1984; accepted 16 February 1984

Seismic Potential Revealed by Surface Folding: 1983 Coalinga, California, Earthquake

Abstract. *The 2 May 1983 Coalinga, California, earthquake (magnitude 6.5) failed to rupture through surface deposits and, instead, elastically folded the top few kilometers of the crust. The subsurface rate of fault slip and the earthquake repeat time are estimated from seismic, geodetic, and geologic data. Three larger earthquakes (up to magnitude 7.5) during the past 20 years are also shown to have struck on reverse faults concealed beneath active folds.*

Identification of past and future earthquake sources is a fundamental goal of earthquake-hazard reduction, the principal strategy is to locate active faults, determine their most recent slip event, and estimate their slip rate and earthquake repeat time. Most active faults are manifested at the earth's surface by displaced young deposits or by fault scarps. Faults that do not reach the surface or do not cut surface deposits are not recognized or are classed as inactive unless they can be independently identified by strain accumulation at the surface or by seismicity at depth.

The 1983 Coalinga, California, earthquake of magnitude (M_s) 6.5 provides a striking illustration of slip on an active but concealed fault that had not been detected by seismic reflection and network microseismicity. We present evidence that the fault slipped about 2 m over a depth of 4 to 12 km, unaccompanied by surface rupture except during one aftershock (*1*, *2*). Despite an estimated 2 km of cumulative fault slip during the past 1 to 2 million years, no major fault scarp has formed. We also consider three other larger and well-studied thrust earthquakes that were accompanied by surface folding and decreased surface rupture in comparison with the slip at depth and contend that, in some tectonic environments, folds form as a consequence of repeated subsurface thrust events. Because the peak ground motion associated with thrust earthquakes appears to be two to three times higher than that observed for normal slip events of the same size (*3*), active folds should be regarded as sites of critical earthquake risk.

Reverse faults that rupture to the earth's surface leave a scarp along the edge of the upthrown fault block; commonly, a prism of sediments accumulates on the downthrown block (Fig. 1, A and B). Whereas slip in great shallow earthquakes, such as the 1906 strike-slip shock on the San Andreas fault in California (*4*), tends to be nearly constant as a function of depth, moderate to large thrust earthquakes typically display less slip at the surface than at depth (*5*). Thrust events that do not extend to the surface deform the rocks above the fault into a gentle fold, do not create a fault scarp, and typically result in the deposition of only a thin veneer of superficial sediments (Fig. 1, C and D). Because most faults in the brittle-elastic layer of the crust cause displacement largely during earthquakes, overlying folds must be built by repeated shocks.

Faults can slip repeatedly without reaching the earth's surface if the stresses at the fault tip and those imposed on the overlying material can relax between earthquakes. Because these stresses can

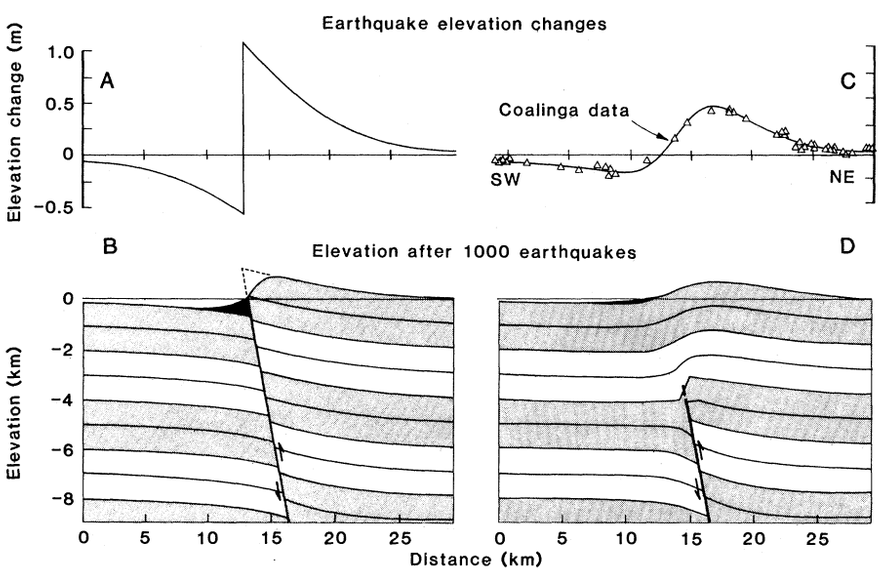

Fig. 1. (A) Elastic dislocation solution for surface deformation caused by 2 m of reverse dip slip on a fault dipping 65° and extending from the ground surface to a depth of 11 km. (B) Depth cross section (vertical exaggeration ×2) after 2 km of cumulative slip, or 1000 earthquakes. Subsequent to initiation of faulting, erosion of fault scarp (dashed) and deposition into downthrown block (black) occur. Remote displacements and interseismic strain release are neglected. (C) Fault shown in (A) terminated 4 km from the surface, except fitted to the observed coseismic elevation changes at Coalinga (*1*). (D) Depth cross section for (C). Dip of beds above the top of the fault increases with depth, and near the top of the fault beds are subject to vertical compression and extension.